Constraining the age distribution of highly mixed groundwater using ^{39}Ar: A multiple environmental tracer (^{3}H/^{3}He, ^{85}Kr, ^{39}Ar, and ^{14}C) study in the semiconfined Fontainebleau Sands Aquifer (France)

J. A. Corcho Alvarado,[1,2] R. Purtschert,[1] F. Barbecot,[2] C. Chabault,[2] J. Rueedi,[3] V. Schneider,[2] W. Aeschbach-Hertig,[4] R. Kipfer,[5] and H. H. Loosli[1]

Received 12 April 2006; revised 28 August 2006; accepted 10 October 2006; published 16 March 2007.

[1] A multitracer (^{3}H/^{3}He, ^{85}Kr, ^{39}Ar, and ^{14}C) approach is used to investigate the age structure of groundwater in the semiconfined Fontainebleau Sands Aquifer that is located in the shallower part of the Paris Basin (France). The hydrogeological situation, which is characterized by spatially extended recharge, large screen intervals, and possible leakage from deeper aquifers, led us to expect a wide range of residence times and pronounced mixing of different water components. Consequently, a large set of tracers with corresponding dating ranges was adopted. Commonly used tracers for young groundwater (^{3}H, ^{3}He, and ^{85}Kr) can identify only those components with ages below 50 years. This approach is reliable if a large fraction of the water recharge occurs within this period. However, if a considerable fraction is older than 50 years, a tracer that covers intermediate age ranges below 1000 years is needed. We examine the use of ^{39}Ar, a noble gas radioisotope with a half-life of 269 years, to constrain the age distribution of groundwater in this timescale range. Recharge rate, depth of water table, and the age structure of the groundwater are estimated by inverse modeling. The obtained recharge rates of 100–150 mm/yr are comparable to estimations using hydrograph data. Best agreement between the modeled and measured tracer concentrations was achieved for a thickness of the unsaturated soil zone of 30–40 m, coinciding well with the observed thicknesses of the unsaturated zone in the area. Transport times of water and gas from the soil surface to the water table range between 10 and 40 and 1 and 6 years, respectively. Reconstructed concentrations of ^{85}Kr and ^{3}H at the water table were used for saturated flow modeling. The exponential box model was found to reproduce the field data best. Conceptionally, this finding agrees well with the spatially extended recharge and large screened intervals in the project area. Best fits between model and field results were obtained for mean residence times of 1–129 years. The ^{39}Ar measurements as well as the box model approach indicate the presence of older waters (^{3}H and ^{85}Kr free). Using ^{39}Ar to date this old component resulted in residence times of the old water components on the order of about 100–400 years. The ^{14}C measurements provide additional evidence for the correctness of the proposed age structure.

Citation: Corcho Alvarado, J. A., R. Purtschert, F. Barbecot, C. Chabault, J. Rueedi, V. Schneider, W. Aeschbach-Hertig, R. Kipfer, and H. H. Loosli (2007), Constraining the age distribution of highly mixed groundwater using ^{39}Ar: A multiple environmental tracer (^{3}H/^{3}He, ^{85}Kr, ^{39}Ar, and ^{14}C) study in the semiconfined Fontainebleau Sands Aquifer (France), *Water Resour. Res.*, *43*, W03427, doi:10.1029/2006WR005096.

[1]Climate and Environmental Physics Division, Physics Institute, University of Bern, Bern, Switzerland.
[2]Laboratoire Interactions et Dynamique des Environnements de Surface, UMR 8148 IDES, Université Paris-Sud, Orsay, France.
[3]Robens Centre for Public and Environmental Health, University of Surrey, Guildford, UK.
[4]Institute of Environmental Physics, University of Heidelberg, Heidelberg, Germany.
[5]Water Resources and Drinking Water, Eidgenössische Anstalt für Wasserversorgung, Abwasserreinigung und Gewässerschutz, Dübendorf, Switzerland.

0043-1397/07/2006WR005096

1. Introduction

[2] Environmental tracer methods are nowadays routine tools for obtaining information about the flow dynamics of groundwater. One of the most important applications is for groundwater dating. Amongst the most frequently used dating tracers we find: ^{3}H/^{3}He [*Schlosser et al.*, 1988, 1989; *Poreda et al.*, 1988; *Solomon and Cook*, 1999], ^{85}Kr [*Smethie et al.*, 1992; *Loosli et al.*, 1999], CFCs [*Busenberg and Plummer*, 1992; *Plummer and Busenberg*, 1999], ^{14}C [*Fontes and Garnier*, 1979; *Mook*, 1980; *Kalin*, 1999]. Other environmental tracers provide information on

the origin and recharge conditions of the groundwater, in particular the stable noble gases [*Mazor*, 1972; *Stute et al.*, 1992; *Stute and Schlosser*, 1999] and the stable isotopes of the water ^{2}H and ^{18}O [*Coplen et al.*, 1999].

[3] Many processes and parameters determine the concentrations of isotopes or chemical tracers in groundwater (e.g., radioactive decay, hydrodynamic dispersion, mixing, chemical degradation, recharge date, transport time through unsaturated and saturated zones, etc.). However, in particular cases factors that lead to a misinterpretation of tracer concentrations in terms of residence time can provide important and additional information such as mixing and dispersion in the aquifer. The interpretation of tracer concentrations is commonly carried out by models that try to mathematically describe the age distribution of sampled groundwater. The estimation of a set of free model parameters requires a corresponding number of measurements. This can be achieved with a high spatial sampling density, by time series at single locations, or by applying multitracer measurements at selected locations, which is the case for the present study. The latter technique is particularly useful to consistently interpret single well measurements.

[4] The study area is located in a semiconfined subsystem of the Paris Basin where the main objective was to determine the age structure of the groundwater. The limited number of sampling sites in the project area requires the application of multiple groundwater dating tracers and the use of lumped parameter approaches for the assessment of groundwater dynamics where the choice of an appropriate age weighting function that appropriately represents the hydrogeological situation can be validated using the measured tracer data. Thus the results of several models can be compared and also the sensitivity of the model to parameters such as the mean residence time (MRT) or recharge rate can be investigated [*Rueedi et al.*, 2005].

[5] The commonly adopted approach for dating and quantifying the portion of young (postbomb) water components is the combination of ^{3}H with either ^{3}He or ^{85}Kr [*Schlosser et al.*, 1989; *Solomon and Cook*, 1999; *Loosli et al.*, 1999]. However, these tracers preferentially detect the "young tail" of age distributions which may include significant amounts of prebomb water. Hence, to verify to which extent the extrapolation of the interpretation with these tracers to the "old tail" fits the real situation in the aquifer an intermediate age (<1000 years) dating technique is required, which is what ^{39}Ar enables in this study. This tracer has been proposed for dating groundwater for its ideal characteristics [*Loosli*, 1983]: a constant and well known atmospheric input concentration, no local contamination, an isotope ratio ($^{39}Ar/Ar$) that is insensitive to degassing or incomplete gas extraction yield, and an important dating range for groundwater hydrology. Argon 39 has been previously used in selected studies [*Oeschger et al.*, 1974; *Andrews et al.*, 1984; *Loosli et al.*, 1989; *Pearson et al.*, 1991; *Loosli et al.*, 1992; *Beyerle et al.*, 1998; *Loosli et al.*, 1999; *Purtschert et al.*, 2001a].

[6] The knowledge of a reliable local input function is crucial for the accurate application of environmental tracers for groundwater dating. These initial concentrations may vary spatially but also as function of the depth of the water table below ground surface [*Cook and Solomon*, 1995]. Absolute as well as relative delays of different tracers become significant in thick unsaturated zones. This is the case in the investigated area with recharge depths between 20 and 40 m. Therefore a one dimensional transport model was integrated in the box model in order to calculate the tracer input at the water table. This procedure introduces additional parameters namely the porosity and tortuosity of the unsaturated soil and the recharge rate. Some of these parameters can be estimated based on complementary methods, others have to be determined by fitting to the tracer data. With the proposed inverse procedure mean recharge rates in the area of investigation can be estimated. The approach presented to investigate parameters in the Fontainebleau Sands Aquifer can be generalized and used for other tracers and for determining parameters at many other sites.

2. Site Characterization

[7] The area of investigation is located in the shallower zone of the Paris Basin (France), which is the largest sedimentary basin of western Europe (Figure 1). The Oligocene sandy aquifer is embedded between two clayey layers (Figure 2): above is the Beauce formation which was altered by diagenesis from limestone to millstone and clay [*Ménillet*, 1988]; and below are Oligocene and Eocene marls which separate the Fontainebleau Sands from the underlying Eocene multilayered aquifer.

[8] Constituted by very fine, well-sorted silica grains with an average diameter of 100 μm, the Fontainebleau Sands formation has a thickness of 50 to 70 m (Figure 2), a hydraulic transmissivity of 1×10^{-3} to 5×10^{-3} m^2/s and a mean total porosity of about 25% [*Mégnien*, 1979; *Mercier*, 1981; *Vernoux et al.*, 2001]. The upper part of the formation is made of up to 99% of pure quartz sands (white facies), while the content of organic matter, carbonates, sulphides, feldspar and clays (dark facies) increases with depth [*Bariteau*, 1996]. It is assumed that the transition of the "white facies" to the "dark facies" is discrete rather than continuous [*Schneider*, 2005].

[9] The mean precipitation rate in the area is about 700 mm/yr (Station Trappes of Meteo France: observation period from 1991 to 2000). The estimated recharge rate varies between 80 and 210 mm/yr based on hydrograph data [*Mercier*, 1981; *Bariteau*, 1996; *Schneider*, 2005]. Groundwater tables of the investigated wells lie between 20 and 45 m below ground level (mbgl) (Table 1). There are at least four different areas with high piezometric heads (Figure 1, modified after *Rampon* [1965]), indicating different flow regimes within the investigated region. The groundwater head distribution is mainly a consequence of the topography where water flows from the elevated plateaux to the lower valleys where groundwater discharges. During recent decades the aquifer has suffered a substantial abstraction to meet the water supply needs of the region. However, water tables decreased only slightly because of the high yield and conductivity of the aquifer.

[10] Nitrate concentrations in groundwater range between 15 and 30 mg/L (European Union, Natural baseline quality in European aquifers—A basis for aquifer management, EC Framework V Project, EVK1-CT1999-0006). These elevated nitrate concentrations, which originate mainly from agricul-

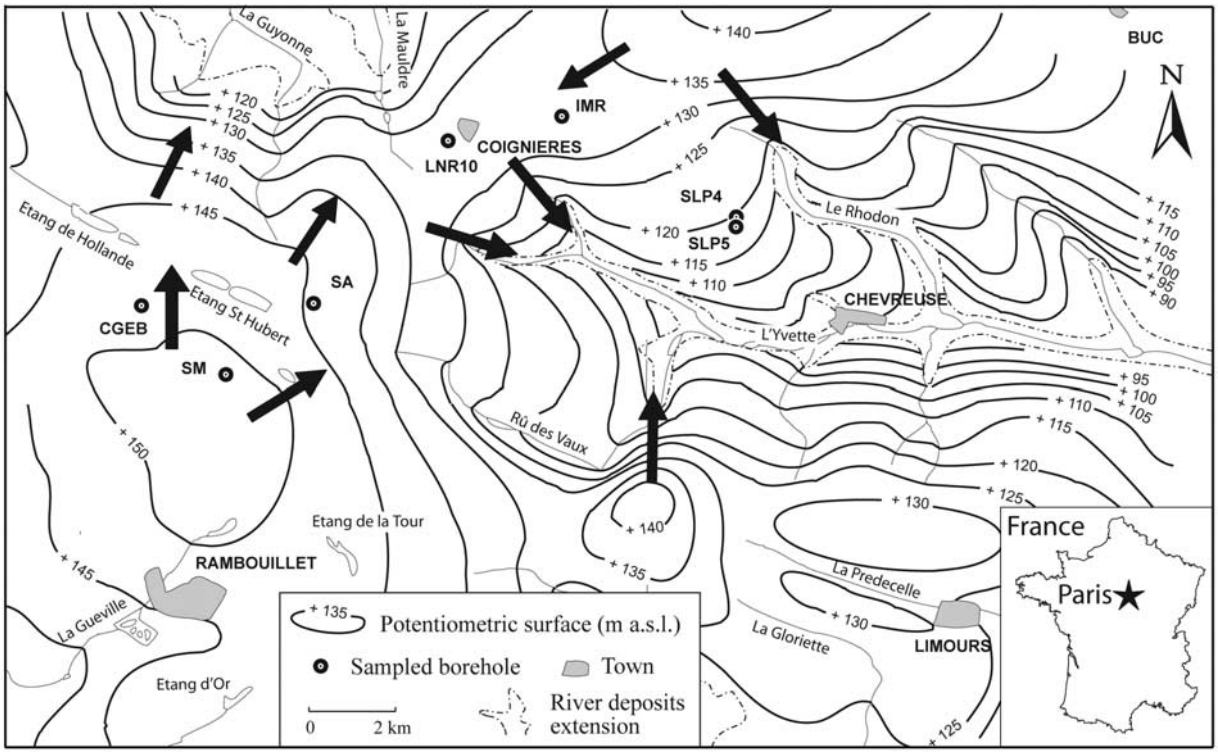

Figure 1. Location of the study area showing the isopiezometric heads in the Fontainebleau Sands Aquifer (modified after *Rampon* [1965]) and the location of the sampling wells. Arrows indicate the most probable flow directions.

ture, point to the vulnerability of the aquifer to surface pollution and the presence of recent water components.

[11] Possible leakage from the underlying Eocene aquifers to the Fontainebleau Sands was indicated in some areas based on sulphate measurements [*Bergonzini*, 2000]. However, in the area of the present investigation, the potentiometric surface of the Eocene aquifer is far below that of the Fontainebleau Aquifer preventing any upward

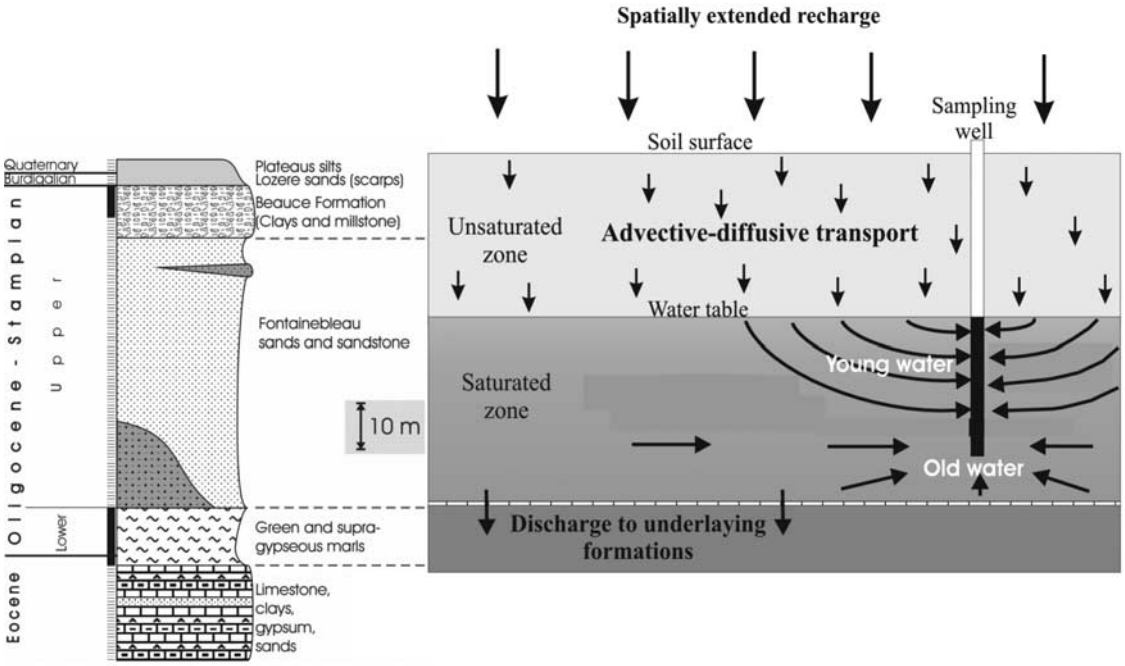

Figure 2. (left) Geological profile of the aquifer and (right) schematic display of the applied conceptual model including the unsaturated zone.

Table 1. Characteristics of the Wells of the Fontainebleau Sands Aquifer Selected for the Investigation[a]

Well	Soil Surface Elevation, masl	Depth of the Water Table In 1965,[b] mbgl	Depth of the Water Table Today, mbgl	Screen Elevation (Present-Day Data), mbgl		
				Screen 1	Screen 2	Screen 3
SM	175.8	25–20	21	21.0–37.9	44.4–46.9	51.0–53.5
CGEB	176.0	31–26	35	35.0–46.1[c]		
SA	171.0	31–26	38	38.0–49.2[c]		
LRN10	171.0	40–35	39	38.5–61.0		
IMR	169.5	40–35	38	46.0–58.0		
SLP4	154.5	40–35	55	55.4–56.0	60.5–61.0	66.8–67.3
SLP5	141.5	26–21	43[c]	50.0–50.5	52.5–53.0	

[a]Groundwater was not abstracted from SM by more than 10 years before the sampling. Here masl is meters above sea level, and mbgl is meters below ground level.
[b]Data from *Rampon* [1965].
[c]Uncertainty in the value of the depth.

seeping through the confining lower Oligocene [*Schneider*, 2005].

3. Methods

3.1. Field and Laboratory Investigations

[12] Seven boreholes from the Fontainebleau Sands Aquifer were sampled in October 2001 for extensive tracer investigation. Most of the sampling points are located in the central part of the aquifer, which is the part most heavily exploited for water supply. It is important to emphasize that the sampled wells are in general screened over a large depth interval of the aquifer and that these screens intercept the water table in most cases (Table 1). Field measurements of pH, dissolved O_2, water temperature and electric conductivity were carried out.

[13] Two to five cubic meters of groundwater were degassed in the field to analyze the radioactive noble gases ^{37}Ar, ^{39}Ar, and ^{85}Kr. In the laboratory, the gases argon and krypton were separated from the samples and ^{39}Ar, ^{37}Ar, and ^{85}Kr activities were measured by low level gas proportional counting in the Deep Laboratory of the Physics Institute, University of Bern, Switzerland [*Loosli*, 1983; *Loosli et al.*, 1986; *Forster et al.*, 1992].

[14] Water samples for noble gas analyses were immediately transferred to 45 ml copper tubes and sealed with pinch-off clamps [*Beyerle et al.*, 2000]. The copper tubes were connected to the point of water withdrawal by flexible plastic tubing secured with hose clamps (gas tight) and the water was flushed for several minutes (until no bubbles were detected in the plastic tube) through the copper tube at high pressures before the steel clamps were closed. The measurements were carried out in the noble gas laboratory of ETH Zurich (Switzerland) according to the procedures described by [*Beyerle et al.*, 2000]. Recharge temperatures (NGTs) are calculated from noble gas concentrations by accounting for their temperature-dependent solubilities and for the common excess air component found in groundwater [*Aeschbach-Hertig et al.*, 1999, 2000].

[15] The measurements of ^{3}H were performed at the Physics Institute of the University of Bern by liquid scintillation counting after an enrichment step. The ^{3}H measurements were combined with the measurements of the decay product ^{3}He to obtain ^{3}H/^{3}He ages [*Schlosser et al.*, 1989]. The ^{3}He concentrations of tritiogenic origin were calculated from the noble gas data [*Beyerle et al.*, 2000].

[16] One liter samples were collected for the analyses of the carbon isotopes (^{14}C and ^{13}C) content of the dissolved inorganic carbon. The radiocarbon activities were measured by AMS (graphite sources, Université Paris-Sud and measurements at Tandetron, Gif sur Yvette) and are expressed as a percentage of modern carbon (pmC). The δ^{13}C contents were measured by mass spectrometry at the IDES Laboratory (Université Paris-Sud) and are expressed in permil variations from the Vienna Peedee Belemnite Standard (‰ VPDB).

3.2. Strategy of Interpretation of Tracer Data

[17] Transient tracers like ^{3}H, ^{3}He and ^{85}Kr are sensitive for young groundwater components with residence times less than about 50 years. Lacking more detailed data in the area of investigation simple age frequency distributions are assumed for these young waters. These so-called box models [*Zuber and Maloszewski*, 2001] are constrained by few parameters like the mean residence time (T_m) and a parameter describing the dispersion of the age distribution (e.g., Pe, η). We can expect consistent results from this approach if the following conditions are fulfilled.

[18] 1. The input concentrations of the tracers at the water table are well known. The local temporal evolution of atmospheric concentrations of ^{3}H, and to a fewer extent ^{85}Kr, are afflicted by some uncertainties. Additionally, tracer input concentrations at the water table depend on the transport mechanisms through the unsaturated soil zone. Helium 3 produced by ^{3}H decay may be lost to a large extent from the unsaturated zone. We assume that these effects are on average similar for all of the investigated wells and that small-scale spatial variations are smoothed out by mixing due to spatially distributed recharge, long screen sampling and dispersion.

[19] 2. The assumed age distribution of water in the aquifer is adequate. Box model age distributions are simple idealizations of complex flow patterns in aquifers [*Zuber and Maloszewski*, 2001]. In the present case the exponential model (EM) seems to be the appropriate approach but also other models have to be examined by sound statistical criteria. Large-scale heterogeneities and multi component mixing can lead to very pronounced age dispersion [*Weissmann et al.*, 2002]. This tailing toward older ages can be examined with a tracer sensitive to water ages older than 50 years. The ^{39}Ar measurements were therefore included in the present investigation.

Table 2. Description of the Lumped Parameter Models, Their Weighting Functions, and Parameters[a]

Lumped Parameter Models	Weighting Function	Parameters
Piston flow model (PFM)	$h(T_m, m) = m \cdot \delta(t - T_m)$	T_m, m
Exponential model (EM)	$h(T_m, t, m) = \frac{m}{T_m} \cdot \exp\left(\frac{-t}{T_m}\right)$	T_m, m
Dispersion model (DM)	$h(T_m, t, Pe, m) = m \cdot \sqrt{\frac{Pe \cdot T_m}{4\pi}} \cdot \left(\frac{1}{t}\right)^{\frac{3}{2}} \cdot \exp\left(\frac{-Pe \cdot (t - T_m)^2}{4 \cdot T_m \cdot t}\right)$	T_m, m, Pe
Exponential piston flow model (EPFM)	$h(T_m, t, \eta, m) = \frac{m \cdot \eta}{T_m} \cdot \exp\left(\frac{-\eta \cdot t}{T_m} + \eta - 1\right)$ for $t \geq T_m(1 - 1/\eta)$, 0 for $t < T_m(1 - 1/\eta)$	T_m, m, η

[a] Tm is the mean residence time, δ is the Dirac delta function (PFM), and η is the ratio of the total volume to the volume with exponential distribution of transit times (η is applied in the EPFM). Pe is Peclet number and defines the relative importance of advective and dispersive flow. (Pe is applied in the DM). Mixing of different groundwater components can potentially occur in the Fontainebleau Sands Aquifer. This mixing requires the introduction of an additional parameter m which accounts for the fraction of younger water (<50 years).

[20] 3. A significant fraction of the water is marked with transient tracer or in other words is younger than 50 years. Very often box models are used together with transient tracers like $^3H/^3He$, ^{85}Kr, SF_6 etc. In this case, the fraction of water that is younger than 50 years defines the sensitivity of the tracer concentrations to the shape of the estimated over all age distribution. Even in the case of an exponential age distribution which weights the youngest waters most the fraction of tracer bearing water is less than 20% if the mean residence time is higher than 220 years. The resulting uncertainties due to the extrapolation to the water portion which contains no modern tracers can again be reduced by ^{39}Ar data.

[21] Our approach of data analyses includes therefore the following stages. A general transport model of unsaturated zone flow (one-dimensional advection-diffusion-decay transport model (1D-ADDTM)) is coupled with lumped parameter models (LPM) for saturated flow at each individual well in the saturated zone. Some parameters of the 1D-ADDTM are known from the literature. Others like a mean unsaturated zone thickness (for all wells) and the recharge rate are included in the inversion procedure as global free parameters. LPM parameters for each well and global parameters are then estimated by a χ^2 fitting routine. Thereby ^3H, ^3He and ^{85}Kr data are treated symmetrically and a priory no tracer or tracer ratio is favored (e.g., the $^3H/^3He$ ratio). The parameters which best explain the data are then checked for consistency with the ^{39}Ar measurements.

[22] All the tracers used in this investigation could be combined in a single fitting step for finding the model parameters that best describe the aquifer conditions; but they are analyzed in a two step approach in order to be able to assess the contribution of ^{39}Ar to the dating of groundwater. In a one step approach the significance of introducing ^{39}Ar measurements in the study is masked by the inverse fitting algorithm. This approach favors the most accurate measurements which are the tritiogenic ^3He concentrations. Hence even if ^{39}Ar is included in the inverse modeling algorithm no significant differences are observed in the fitting results.

3.2.1. Lumped Parameter Models and Input Function

[23] The LPM is given by a weighting function $h(t, p_j)$ with parameters p_j which describe the age distribution of the water (Table 2). The convolution of tracer input c_{in} to tracer output c_{out} for a certain sampling date T_s is calculated according to the formula,

$$c_{out}(T_s, p_j) = \int_0^\infty c_{in}(T_s - t) \cdot \exp(-\lambda t) \cdot h(t, p_j) \cdot dt \qquad (1)$$

where t is the integration time, λ is the decay constant and p_j are the model parameters given in Table 2. A more detailed description of the LPM is given by *Zuber* [1986] and *Zuber and Maloszewski* [2001].

[24] It is crucial to select or determine the correct input function in equation (1). The atmospheric activities of ^{85}Kr are measured routinely at Freiburg (Institute of Atmospheric Research (IAR), Freiburg, Germany). These activities have been taken as the ^{85}Kr input function in several groundwater studies. However, direct measurements of ^{85}Kr in soil gas samples from the unsaturated zone (USZ) of the Fontainebleau sands aquifer and in air samples in the region of location of the aquifer revealed activities consistently 1.4 times higher than those measured in Freiburg [*Corcho Alvarado et al.*, 2004]. Such elevated values can be attributed to the proximity to the main ^{85}Kr emission sources in Europe La Hague and Sellafield [*Corcho Alvarado et al.*, 2004]. Therefore the ^{85}Kr atmospheric activities measured at Freiburg were multiplied by a correction factor of 1.4 in order to estimate the input function at the soil surface in the Fontainebleau area. This scaling factor agrees with results from atmospheric circulation model calculations [*Winger et al.*, 2005] based on worldwide ^{85}Kr emission data (e.g., nuclear reprocessing plants).

[25] The ^3H input was constructed averaging the ^3H fallout data reported for the stations located in Le Mans and Orleans-La-Source (data taken from IAEA/WMO Global Network of Isotopes in Precipitation database, http://isohis.iaea.org). A value of 5 TU was assumed for water recharged prior to the bomb tests [*Roether*, 1967].

[26] In confined aquifers with long groundwater residence times and comparably short transit times through the USZ, the delay of environmental tracers in the USZ can be neglected [*Cook and Solomon*, 1995]. In these cases the atmospheric concentrations of the tracers can be used as input values for the modeling. However this simplification is probably not valid in the case of the Fontainebleau Sands Aquifer because of the extended USZ with a thickness of

Table 3. Parameters Used for the One-Dimensional Advection-Diffusion Decay Transport Model

Parameter	Value	Free or Fixed
Water filled porosity θ_l	0.1[a]	fixed
Gas filled porosity θ_g	0.15[a]	fixed
Dispersivity α	0.1 m[b]	fixed
Tortuosity in the gaseous phase τ_g	0.6[c]	fixed
Tortuosity in the liquid phase τ_l	0.25[d]	fixed
Recharge rate q_l	50–500 mm/yr[a]	free
Recharge depth Z	20–40 mbgl	free

[a]*Mégnien* [1979], *Vernoux et al.* [2001], and *Schneider* [2005].
[b]*Cook and Solomon* [1995].
[c]*Millington* [1959].
[d]*Barraclough and Tinker* [1982].

20 to 45 m (Figure 2 and Table 1). Therefore transport times of tracers through the USZ have to be taken into account when dating young groundwater components [*Cook and Solomon*, 1995]. While water-bound tracers like ^{3}H are transported mostly advectively with the water seepage, the transport of gaseous tracers (^{85}Kr) is mainly diffusion controlled within the unsaturated soil pores. The very volatile ^{3}He produced by decay of ^{3}H is quantitatively lost to the atmosphere [*Schlosser et al.*, 1989].

[27] A one-dimensional advection-diffusion-decay transport model was used to simulate the ^{85}Kr and ^{3}H concentrations C in the USZ as function of depth z and particularly to estimate their concentrations above the groundwater table [*Cook and Solomon*, 1995; *Rueedi et al.*, 2005]. Assuming homogeneous physical conditions throughout the USZ, the mass balance differential equation can be expressed as

$$\frac{\partial C_l}{\partial t} = D^* \cdot \left(\frac{\partial^2 C_l}{\partial z^2}\right) - q^* \cdot \left(\frac{\partial C_l}{\partial z}\right) - \lambda \cdot C_l \qquad (2)$$

with

$$D^* = \frac{\left(D_l \cdot \rho_l + D_g \cdot \rho_g \cdot K\right)}{\theta^*} \qquad \left[\mathrm{m^2/yr}\right]$$

$$q^* = \frac{q_l \cdot \rho_l}{\theta^*} \qquad \left[\mathrm{m/yr}\right]$$

$$\theta^* = \theta_l \cdot \rho_l + \theta_g \cdot \rho_g \cdot K \qquad \left[\mathrm{kg/m^3}\right]$$

where $C_g = K \cdot C_l$, θ_l and θ_g are the water filled and the gas filled porosities, respectively, λ is the decay constant of the radioisotopes [yr^{-1}], ρ is the density [g/cm^3], q_l is the advective flow velocity [m/yr], D is the diffusion coefficient in the gaseous (g) and liquid (l) phase respectively [m^2/yr], and K is the equilibrium partition coefficient between the liquid and gas phase. Note that an instantaneous equilibration between the two phases is assumed.

[28] The diffusion coefficients D, in the water and gas phase are estimated by

Gas phase

$$D_g = D_g^o \cdot \theta_g \cdot \tau_g \qquad \left[\mathrm{m^2/yr}\right]$$

Liquid phase

$$D_l = D_l^o \cdot \tau_l \cdot \theta_l + \alpha \cdot \frac{q_l}{\theta_l} \qquad \left[\mathrm{m^2/yr}\right]$$

where D^o is the self-diffusion coefficient of the species in air (g) and in water (l); $\tau_{g\ or\ l}$ are the gaseous (g) and liquid (l) tortuosity (value: $0 < \tau_{g\ or\ l} < 1$); and α is the dispersivity [m].

[29] Equation (2) was solved using an implicit Crank-Nicholson scheme. The upper and lower boundary conditions are given by the atmospheric input concentration at the soil surface and zero diffusive flux at the water table in depth Z [*Rueedi et al.*, 2005]. The latter condition is justified by the fact that the diffusion coefficient D^* drops by about four orders of magnitude at the groundwater surface. A detailed description of the numerical solution is given by *Rueedi et al.* [2005].

[30] According to sensitivity analysis performed by *Rueedi et al.* [2005], the parameters that most strongly influence the model results for the water dominated tracer ^{3}H are the water filled porosity (θ_l); the dispersivity (α); and the recharge rate (q_l). The gaseous tracer ^{85}Kr is most sensitive to the diffusion coefficient in the gas phase which depends on the gas filled porosity (θ_g) and tortuosity (τ_g). Data from the literature were used to better constrain the soil parameters used in the 1D-ADDTM. Values of about 0.10 for θ_l and of about 0.25 for the total porosity were reported for this formation [*Mégnien*, 1979; *Vernoux et al.*, 2001; *Schneider*, 2005]. The dispersivity α was set to 0.1 m [*Cook and Solomon*, 1995; *Rueedi et al.*, 2005; *Gaye and Edmunds*, 1996]. The tortuosities are assumed to be about 0.6 for the gaseous phase [*Millington*, 1959] and about 0.25 for the liquid phase [*Barraclough and Tinker*, 1982].

3.2.2. Inverse Fitting Procedure

[31] Estimates of the parameters θ_l, θ_g, τ_g, τ_l and α of the 1D-ADDTM are reasonable known in the Fontainebleau Sands Aquifer (Table 3) and were fixed in the calculations. On the other hand, estimated values of the recharge rate q_l in the area of investigation vary between 80 and 210 mm/yr [*Mercier*, 1981; *Bariteau*, 1996; *Schneider*, 2005]. This parameter was therefore included in the fitting as a global variable and was allowed to vary in a range between 50 and 500 mm/yr. The thickness of the unsaturated soil zone is known at each well. However, recharge occurs spatially distributed potentially at any location between the wells. It was decided to select the mean recharge depth Z also as a global fitting parameter varying manually in the observed range between 20 and 40 m.

[32] The combination of the LPM with the 1D-ADDTM can be described by a vector of free parameters *mod* containing 2 global (q_l, Z) and n p parameters where n is the number of sampling sites (in our study case n = 7) and p depends on the LPM selected (p = 2 for EM, p = 3 in for DM and EPM, Table 2).

$$mod = \left[q_l, Z, T_{m,i}, mi, \eta_i\ or\ Pe_i\right] \qquad \mathrm{i : 1..n}$$

and the measured tracer data for n wells as a vector *data* of $3 \cdot$ n parameters,

$$data = \left[\mathrm{C}\left(^3\mathrm{H}\right)_\mathrm{i},\ \mathrm{C}\left(^3\mathrm{He}\right)_\mathrm{i},\ \mathrm{C}\left(^{85}\mathrm{Kr}\right)_\mathrm{i}\right] \quad \mathrm{i : 1..n}$$

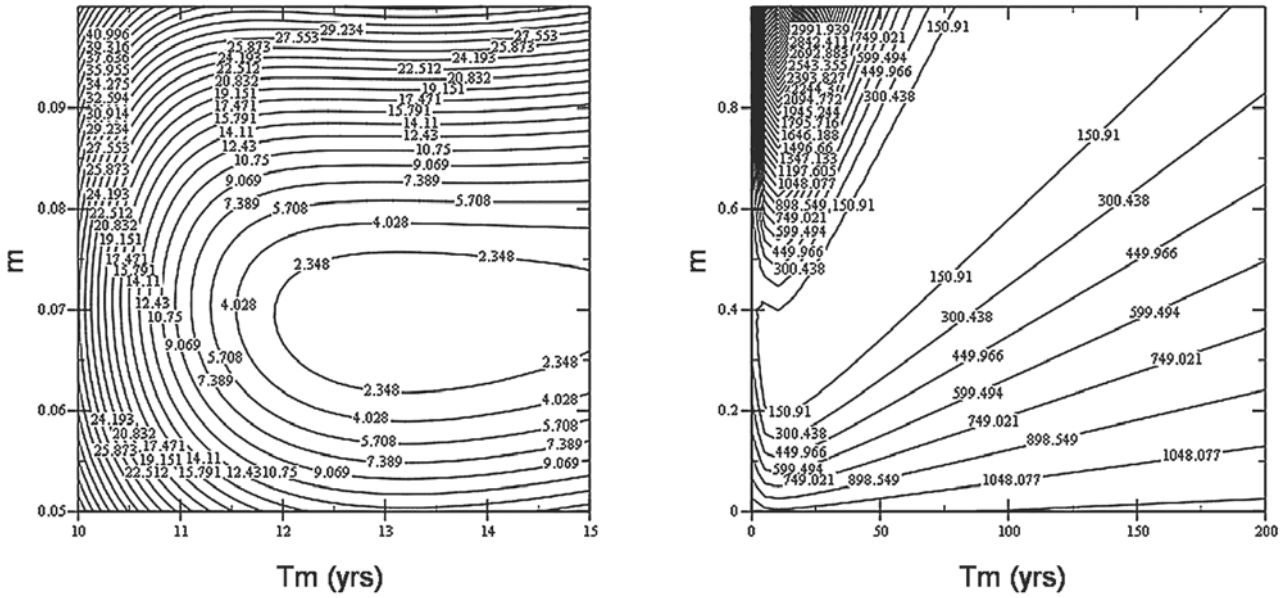

Figure 3. Contour plots of the χ^2 surface in the parameter space calculated for the tracer data of the wells (left) IMR and (right) LRN10, with the EM assuming the water table at 35 mbgl and a recharge rate of 150 mm/yr. In the first case, the χ^2 surface is circular and a well-defined minimum is obtained. The parameters that best fit the EM to the tracer data are $T_m = 13 \pm 1$ years and $m = 0.07 \pm 0.01$. In the second case, the model parameters show a strong correlation, and the confidence interval of the parameters become large. The parameters that best fit the EM to the tracer data are $T_m = 129 \pm 454$ years and $m = 1.0 \pm 1.0$.

[33] The parameters *mod* that best fit the LPM to the observation data are estimated by minimizing the χ^2 function:

$$\chi^2 = \sum_i^n \sum_y^3 \frac{\left(C^y_{i,measured} - C^y_{i,\mathrm{mod}}\right)^2}{\delta_i^{y^2}} \qquad (3)$$

where $C^y_{i\,measured}$ are the measured tracer concentrations (y = ^{85}Kr, ^{3}H or ^{3}He; and i = 1..n), δ^y_i is the error of the measurements and $C^y_{i\,mod}$ are the concentrations predicted by the LPM after convoluting the input concentrations of the tracers calculated with the 1D-ADDTM. Weighting with $1/\delta_i^{y2}$ favors accurate measurements in the fitting routine [*Press et al.*, 1986; *Aeschbach-Hertig et al.*, 1999]. The number of degrees of freedom F of the χ^2 distribution is defined by $F = N - M$, where N is the number of measurements (n · 3 = 21) and M the number of free parameters of the model (EM: 2 · n + 2 = 16 → F = 5; DM, EPM 3 · n + 2 = 23 → F = −2). The system is under defined for the DM and the EPM because the number of free parameters is higher than the number of measurement (F < 0). Because of the homogeneity of the sands and the similarity of the hydraulic conditions over the area of investigations, it can be assumed that the Peclet number Pe or the parameter η are similar for all wells. These parameters were therefore also selected as a global free parameter resulting in F = 4 for the EPM and the DM.

[34] This inverse approach offers the possibility of an error estimation of the fitted model parameters. They are calculated from the covariance matrix based on the propagation of the experimental errors [*Press et al.*, 1986; *Aeschbach-Hertig et al.*, 1999].

[35] Correlation between parameters leads to large uncertainties of the estimation of these parameters [*Aeschbach-Hertig et al.*, 1999; *Press et al.*, 1986]. This can be visualized in a contour plot of the χ^2 surface of an individual sample (Figure 3). Residence time T_m and mixing portion m are, e.g., correlated for timescales when an increase of residence time (more water above the 50 years limit) can be compensated by a corresponding increase of the young water portion or vice versa. In such cases the parameters cannot be resolved without constraining one of them [*Poeter and Hill*, 1997; *Carrera et al.*, 2005] or by adding further constraints such as ^{39}Ar measurements. The reconstructed ^{39}Ar activity originating from the water components dated by ^{85}Kr, ^{3}H and ^{3}He must be, within uncertainties, (1) equal or (2) smaller than the measured ^{39}Ar activities. In case 1 the whole water mass can be described by the LPM. In case 2 and if the mixing ratio of young water m < 1, additional water components contributing to the whole water mass have to be assumed. If neither case 1 nor 2 are fulfilled the fit has to be rejected.

4. Results and Discussion

[36] ^{85}Kr and ^{3}H were detected at all sampling sites at levels well above the detection limits, indicating the presence of modern water. Measured concentrations of ^{3}H vary from 3.1 to 15.1 TU, and the specific activities of ^{85}Kr show large variation between 2.9 and 43.0 decays per minute (dpm)/cm^3 STP Kr (Table 4). The noble gas composition of the water samples are presented in Table 5. In general, the interpretation of noble gas concentrations, which is

Table 4. Radioactive and Stable Isotope Measurements and Calculated Apparent Tracer Ages Assuming PF and EM

	Data					PF Ages, years			EM Ages, years	
Well	^{85}Kr, dpm/cm^3 Kr	^{3}H, TU	^{39}Ar, % modern	^{14}C, pmC	^{13}C, ‰ versus VPDB	^{3}H/^{3}He	^{85}Kr	^{39}Ar	^{85}Kr	^{39}Ar
SM	43.0 ± 5.0	10.0 ± 0.8	79 ± 7	80.2 ± 0.6	−16.3	8 ± 1	11 ± 1	91 ± 35	11 ± 2	103 ± 45
CGEB	6.8 ± 0.7	8.5 ± 0.8	73 ± 5	75.1 ± 0.6	−14	9 ± 1	29 ± 1	122 ± 27	122 ± 3	144 ± 37
SA	16.1 ± 4.1	15.1 ± 0.8	69 ± 5	84.2 ± 0.6	−14.3	11 ± 1	20 ± 2	144 ± 28	46 ± 4	174 ± 41
LRN10	6.1 ± 4.8	7.8 ± 0.8	77 ± 5	73.7 ± 0.6	−14.1	15 ± 1	30 ± 5	101 ± 25	137 ± 10	116 ± 33
IMR	2.9 ± 0.4	3.1 ± 0.8	55 ± 5	69.8 ± 0.6	−13.8	9 ± 2	35 ± 1	232 ± 36	299 ± 2	318 ± 65
SLP4	6.2 ± 2.5	7.8 ± 0.8	59 ± 5	75.5 ± 0.6	−13.9	2 ± 1	30 ± 3	205 ± 33	335 ± 30	270 ± 56
SLP5	5.6 ± 2.8	4.0 ± 0.8	51 ± 5	73.8 ± 0.6	−13.7	13 ± 2	31 ± 5	261 ± 38	150 ± 25	373 ± 76

described in more detail in Appendix B, provides evidence that degassing of atmospheric gases within the aquifer is most probably not a significant process. Tritiogenic ^{3}He (^{3}He$_{trit}$) concentrations, NGT and excess air components were calculated based on a model that assumes that excess air is pure atmospheric air (unfractionated air or UA model). However, a model that assumes partial diffusive reequilibration (PR model) and accounts for excess air fractionation also provides acceptable fits, with results that do not differ significantly from those calculated with the UA model. The PR model yields a fractionation parameter F of at most 0.17, equivalent to a maximum loss of 16% of the excess air Ne and 28% of the excess air He (Appendix B).

[37] The ^{39}Ar activities range between 51 and 79% modern, while ^{14}C activities lie between 69 and 84 pmC (Table 4). The relatively high ^{85}Kr and ^{3}H concentrations together with relatively low ^{39}Ar values are clear indications for pronounced mixing of water components with different ages. PF and EM ages deduced from ^{39}Ar activities alone range between 91 and 261 years and 103 and 373 years, respectively (Table 4). Subsurface production of ^{39}Ar, which most probably can be neglected in this aquifer (Appendix A), would shift these ages to even older values. In any case, it can be assumed that a considerable fraction of water in the investigated wells must be older than 50 years and is therefore free of ^{85}Kr and ^{3}H.

[38] In a first step, the modern tracers (^{3}H, ^{3}He$_{tri}$ and ^{85}Kr) are used to identify, quantify and date the young groundwater components present in the aquifer. This first part is performed following the methodology presented in section 3. Then in a second step, ^{39}Ar is used for cross checking these results and to date the old groundwater components that do not contain modern tracers (water that recharged before the year 1950). Additionally, measurements of ^{14}C were used to further constrain the ages of the old groundwater components.

4.1. Young Residence Time Indicators

[39] Tracer concentrations and calculated apparent ages are given in Table 4. The ^{3}H/^{3}He ages τ scatter mostly around 10 years and do not exceed 15 years whereas ^{85}Kr ages vary between 11 and 35 years. For comparison also ^{39}Ar PF ages are given which are significantly higher in the range 90–260 years. This is exactly what can be expected for wide age distributions with a large spreading of ages like the EM [*Waugh et al.*, 2003]. Youngest ages result from ^{3}H/^{3}He ratios because these are unaffected by the admixture of tracer free old water. Tracers with smaller half live result in younger apparent ages than tracers with a higher half-life. The ^{85}Kr and ^{39}Ar ages do agree much better if they are interpreted in the frame of the EM. In Figure 4 ^{3}H/^{3}He ages (τ are plotted as function of the mean EM ^{39}Ar age (T_m). The two curves shown were calculated with the atmospheric ^{3}H values (solid line) and with the input values calculated with the 1D-ADDTM at the water table in 35 depth. The time difference between the two lines corresponds to the transit time of the water through the USZ from where ^{3}He is lost to the atmosphere. Despite some scattering our data follow the theoretical expectations which are based on (1) pronounced mixing (EM) including post bomb water components, (2) different time lags of ^{3}H and ^{85}Kr and ^{39}Ar in the USZ (Figure 5), and (3) degassing of ^{3}He from the USZ into the atmosphere. Outliers like SLP4 require further considerations based on all tracer data.

[40] In Figure 5, the results of modeling the tracer transfer through the USZ for the specific case of a water table at 25 m depth and a recharge rate of 150 mm/yr are presented. The ^{3}H input at the water table is smoothed out and flat

Table 5. Noble Gas Data, Noble Gas Temperatures Obtained With the Unfractionated Air Model, the Amount of Excess Air Expressed as ΔNe, and the ^{3}He Concentration of Tritiogenic Origin[a]

Well	[He], 10^{-8}	^{3}He/^{4}He, 10^{-6}	[Ne], 10^{-7}	[Ar], 10^{-4}	[Kr], 10^{-8}	[Xe], 10^{-8}	χ^2	Probability, %	NGT, °C	ΔNe, %	^{3}He$_{trit}$, 10^{-14}	^{3}He$_{trit}$, TU	He Radiogenic, 10^{-9} cm^3/g
SM	6.45	1.57	2.71	4.18	9.50	1.34	0.18	91.3	9.68 ± 0.21	36.9	1.29 ± 0.08	5.2 ± 0.3	−2.7 ± 0.9
CGEB	6.00	1.61	2.58	4.09	9.36	1.33	0.44	80.4	9.84 ± 0.22	30.5	1.44 ± 0.05	5.8 ± 0.2	−2.0 ± 0.9
SA	6.12	1.87	2.61	4.08	9.32	1.32	0.65	72.3	10.08 ± 0.22	32.0	3.09 ± 0.08	12.4 ± 0.2	−2.3 ± 0.9
LRN10	6.65	1.75	2.77	4.20	9.53	1.35	0.77	68.0	9.59 ± 0.21	39.4	2.56 ± 0.08	10.3 ± 0.3	−1.3 ± 0.9
IMR	7.45	1.44	3.13	4.33	9.54	1.32	0.03	98.6	10.51 ± 0.23	58.9	0.52 ± 0.05	2.1 ± 0.2	−4.2 ± 1.1
SLP4	6.49	1.40	2.76	4.17	9.39	1.32	0.06	97.0	10.27 ± 0.21	39.6	0.17 ± 0.05	0.7 ± 0.2	−3.2 ± 1.0
SLP5	6.67	1.53	2.84	4.18	9.27	1.31	0.52	77.0	10.63 ± 0.22	44.2	1.10 ± 0.05	4.4 ± 0.2	−3.7 ± 1.0
1σ error	0.03	0.01	0.03	0.02	0.14	0.01							

[a]Concentrations are expressed in cm^3 STP of gas per gram of water. NGT, noble gas temperature; UA, unfractionated air model.

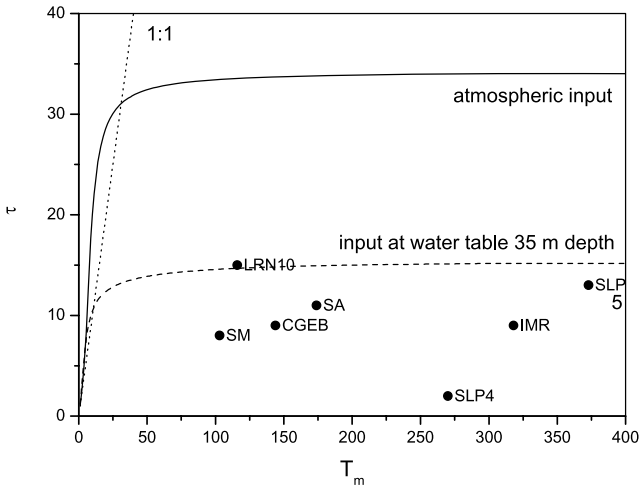

Figure 4. The $^3H/^3He$ ages (τ) plotted as function of the mean residence time T_m of the EM age distribution (ages derived from the ^{39}Ar data). The two curves given were calculated with the EM using as input: (1) the atmospheric ^3H values (solid line) and (2) the input ^3H values calculated with 1D-ADDTM for a water table at 35 mbgl.

compared to the atmospheric fallout curve mainly due to dispersion and radioactive decay. The resulting transport times of ^{85}Kr and ^3H through the USZ range between 1 and 6 years and 10 and 40 years, respectively depending on the water table depth and the recharge rate. Since ^3H is a part of the water molecule, its time lag represents the average transport time of the water from the surface to the water table.

[41] Best fits for ^3H, ^3He and ^{85}Kr according to the procedure explained in section 3 are listed in Table 6 in order of increasing values of the total χ^2. The best results could be obtained with the EM, DM and EPFM. The PFM leads to larger deviations between the modeled and observed values, in agreement with expectation. Best estimates of the parameters recharge rate (q_l) and unsaturated zone thickness Z are in the ranges 100–150 mm/yr and 30–40 m, respectively. The range of the recharge depth agrees well with the hydrogeological boundary conditions in the area. Moreover, the best estimate of spatially averaged recharge rate for the aquifer (100–150 mm/yr) is comparable to previous estimates of this parameter based on hydrological balances (80–210 mm/yr) [*Mercier*, 1981; *Bariteau*, 1996; *Schneider*, 2005]. This agreement can, if the previous estimates are true, be regarded as additional evidence that the assumptions which were made for the unsaturated zone transport are correct.

[42] Mean residence time and mixing ratios obtained from the EM, DM and EPFM do agree in most cases within the calculated errors. This is not surprising if the global fitting parameters Pe and η are considered. The low best fit Pe number and a best fit η parameter close to 1 are both synonymous with an age distribution very similar to the EM. The inverse modeling procedure converges therefore for all assumed models to an EM age distribution, in agreement with the expectations. This demonstrates that multi tracer data can be used to constrain age distributions in cases when the appropriate model is less straight forward. However, one has to keep in mind that other more complex age distribution may lead to an even better agreement between the model and the data. Rather surprising results are the relatively low residence times T_m and mixing fractions m of the young water components following the EM and being responsible for the observed concentrations of ^3H, ^3He and ^{85}Kr. This suggests that a considerable portion of the water is older than 50 years. This can be explained by a two (or multi) component mixing of water originating from different sources or by an age distribution with a more pronounced tailing toward older ages. In some cases it is not possible to constrain T_m and m because these parameters

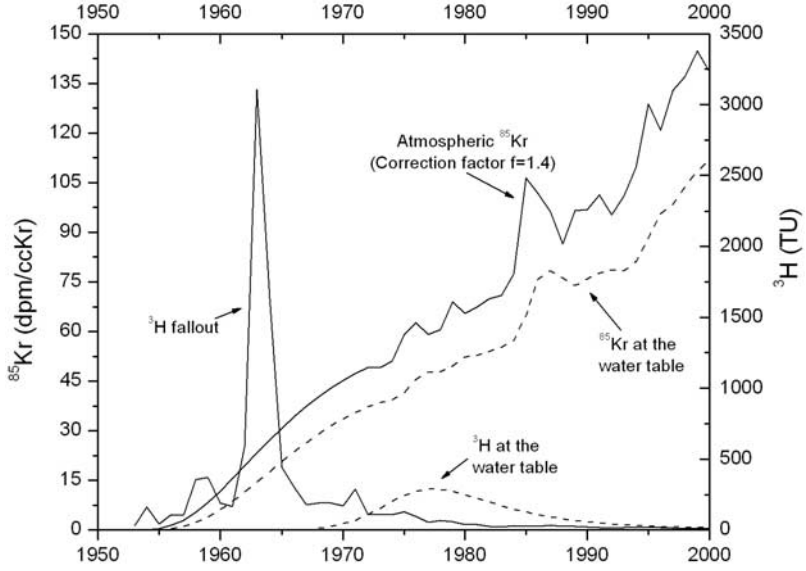

Figure 5. Temporal course of atmospheric ^3H and ^{85}Kr concentrations compared with calculated input concentrations at the water table in 35 m depth. The atmospheric values of ^3H were reconstructed from nearby monitoring stations (GNIP: IAEA database) whereas ^{85}Kr measurements from Freiburg (IAR) were upscaled by a factor of 1.4. The calculations at the water table are based on the transport parameters given in Table 3.

Table 6. Fitting Results of Different Lumped Parameter Models[a]

		Model Parameters				Correlation Factor			
Sample	χ^2	T_m, years	Pe	m	η	T_m _ Pe	T_m _ η	T_m _ m	Pe _ m	η _ m
EM, Recharge Depth of 35 mbgl and Recharge Rate of 150 mm/yr										
CGEB	12	11 ± 2		0.16 ± 0.01				−0.367		
SM	14	4 ± 1		0.36 ± 0.03				0.759		
SA	1	10 ± 1		0.40 ± 0.02				−0.827		
LRN10	0	129 ± 454		1.0 ± 1.0				1.000		
IMR	3	13 ± 1		0.07 ± 0.01				0.065		
SLP4	44	1 ± 1		0.17 ± 0.02				−0.006		
SLP5	0	11 ± 4		0.11 ± 0.01				0.860		
χ^2_T	74									
EM, Recharge Depth of 40 mbgl and Recharge Rate of 150 mm/yr										
CGEB	18	15 ± 3		0.19 ± 0.01				0.765		
SM	4	5 ± 1		0.27 ± 0.02				−0.748		
SA	9	22 ± 7		0.51 ± 0.07				0.985		
LRN10	0	90 ± 185		1.00 ± 1.00				0.999		
IMR	2	7 ± 2		0.05 ± 0.01				0.089		
SLP4	41	1 ± 1		0.16 ± 0.02				−0.131		
SLP5	0	42 ± 86		0.22 ± 0.30				0.999		
χ^2_T	74									
EPFM, Recharge Depth of 35 mbgl and Recharge Rate of 100 mm/yr										
CGEB	11	22 ± 10		0.39 ± 0.27	1.5 ± 2.5		−0.945	0.999		−0.941
SM	48	5 ± 1		0.29 ± 0.02	1.5 ± 2.5		−0.949	0.286		−0.043
SA	1	18 ± 3		0.70 ± 0.37	1.5 ± 2.5		−0.949	0.984		−0.989
LRN10	6	27 ± 18		0.98 ± 0.76	1.5 ± 2.5		−0.981	0.990		−0.944
IMR	21	45 ± 48		0.95 ± 0.80	1.5 ± 2.5		−0.998	0.988		−0.980
SLP4	14	1 ± 1		0.10 ± 0.14	1.5 ± 2.5		−0.905	−0.181		0.581
SLP5	12	11 ± 2		0.19 ± 0.06	1.5 ± 2.5		−0.833	0.925		−0.965
χ^2_T	113									
DM, Recharge Depth of 30 mbgl and Recharge Rate of 100 mm/yr										
CGEB	56	24 ± 14	0.02 ± 0.01	0.26 ± 0.28		0.358		0.993	0.246	
SM	39	6 ± 2	0.02 ± 0.01	0.22 ± 0.02		−0.089		−0.755	0.051	
SA	1	10 ± 1	0.02 ± 0.01	0.70 ± 0.02		0.397		−0.120	0.773	
LRN10	2	34 ± 59	0.02 ± 0.01	0.90 ± 1.00		0.813		0.996	0.757	
IMR	26	42 ± 64	0.02 ± 0.01	0.24 ± 0.60		0.498		0.972	0.282	
SLP4	20	1 ± 1	0.02 ± 0.01	0.13 ± 0.02		−0.000		−0.129	0.000	
SLP5	1	11 ± 2	0.02 ± 0.01	0.09 ± 0.01		0.196		−0.593	0.499	
χ^2_T	145									

[a]Mean residence time (T_m) and mixing ratio (fraction of young water, m) that best fit the EM, the EPFM (η is also shown), and the DM (Pe is also shown) to the measurements of ^{3}H, ^{3}He and ^{85}Kr. The χ^2_T of the fits and the correlation between the calculated parameters are also reported.

are not independent. This is, e.g., the case for the Sample LRN10 (EM and DM). This results in large errors of the fitting parameters although χ^2 is excellent. This emphasizes the need of an additional tracer.

[43] Modeled and measured tracer concentrations for the best fits are compared in Figure 6. In general there is an excellent agreement. Deviations are most probably the result of an averaging of some parameters which is intrinsic in the selection of global parameters. The relatively larger disagreement for ^{85}Kr (correlation factor: R = 0.87) compared to $^3He_{trit}$ (R = 1) is a result of the higher analytical errors of ^{85}Kr measurements and the corresponding lower weight in the fitting procedure (equation (3)).

4.2. Older Water Components Investigated Using ^{39}Ar and ^{14}C

[44] The environmental tracers ^{39}Ar ($T_{1/2}$ = 269 years) and ^{14}C ($T_{1/2}$ = 5730 years) are suitable for a more detailed characterization of the older tail of the age distribution.

[45] In Figure 7, ^{39}Ar is shown as function of ^{85}Kr, ^{3}He and ^{3}H concentrations. The curves plotted in Figure 7 correspond to the theoretical relation when the whole water mass (m = 1) follows the EM. The calculations are based on the atmospheric input (dashed line) and the input values according to the fitting procedure at depth 35 m (solid line). The tracer results of the samples LRN10 and SLP5 are within uncertainties consistent with the EM. In the fitting routine a high correlation between T_m and m caused large errors of the estimated model parameters for these two samples. The ^{39}Ar measurements reduce this large range of solutions and result in mean EM ages T_m of 116 and 373 years, respectively.

[46] The assumption of a one-component EM distribution is obviously not valid for samples SA and SM. At least two young residence time indicators (^{85}Kr, ^{3}H or ^{3}He) predict concurrently, in comparison with ^{39}Ar, an at least bi modal age distribution for SA and SM. The ''young'' end-members of the mixing lines indicated in Figure 7 are based on the age of the young components estimated by the fitting routine. The extrapolated age of old component is about 300–400 years. At least for SM this multimode age distribution could be the result of the separated screen intervals in this well (Table 1). Because both wells are situated in the same section of the area of investigation it is also possible that permeability variations in the sands in this

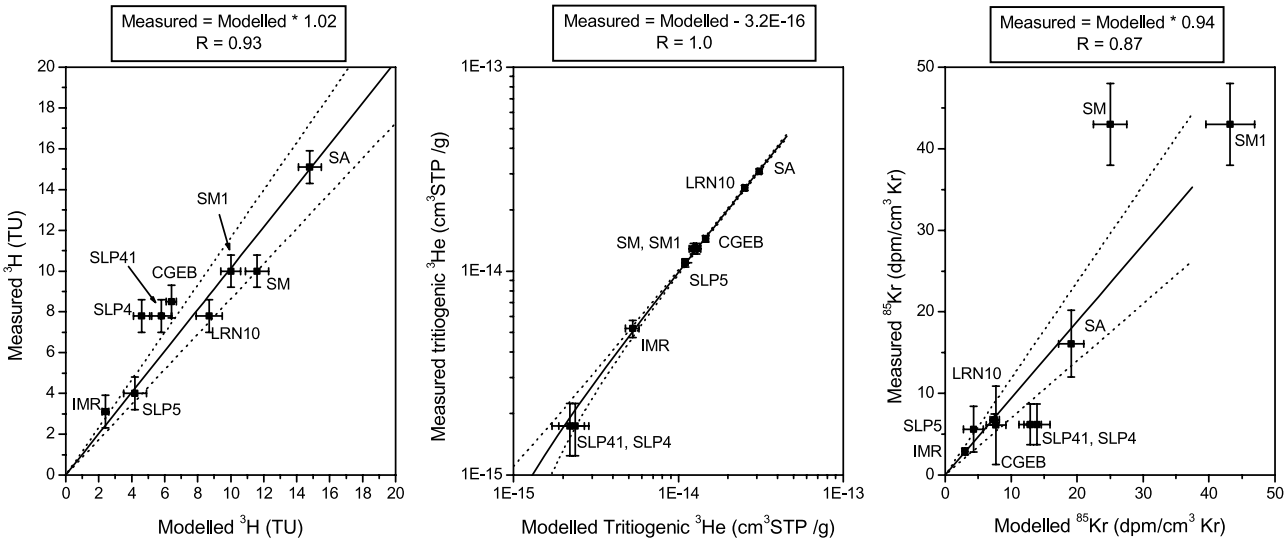

Figure 6. Comparison between the modeled (obtained with the EM) and the measured concentrations of ^{3}H, ^{3}He, and ^{85}Kr. Larger disagreements are observed in samples SM and SLP4. Better agreements are observed at SM and SLP4 when a shallower recharge depth of 20 mbgl and a deeper recharge depth of 40 mbgl are assumed, respectively. The points SM1 (at 20 mbgl) and SLP41 (at 40 mbgl) represent these conditions.

section cause a separation of water bodies with different ages.

[47] In the frame of a pure EM scenario $^3He_{trit}$ tends to be too low for the wells SLP4, IMR and CGEB. Two explanations appear to be the most plausible for this observation.

[48] 1. Helium 3 is the most sensitive tracer for variations of the thickness *Z* of the unsaturated soil zone as can be seen in Figure 7 from the large difference of the two model curves (Z = 0 and Z = 35 mbgl). In comparison the ^{3}H and ^{85}Kr model curves vary only slightly for ^{39}Ar activities below 85% modern. Z was assumed to be similar for all of the wells and was therefore selected as a global fitting parameter in the calculations. Adjusting Z for each individual well would improve in particular the agreement of the ^{3}He data in the frame of a pure EM. With other words: The calculation of ^{3}H/^{3}He EM ages in the saturated soil zone strongly depends on the transit time of water through the unsaturated soil zone (see also Figure 5).

[49] 2. Incomplete confinement of ^{3}He in the saturated zone. This would cause depleted concentrations compared to the less volatile tracers ^{3}H and ^{85}Kr. The lowest value of $^3He_{tri}$ to be expected for prebomb water is 4–5 TU if ^{3}H delay in the unsaturated zone and mixing are neglected, and 1 TU if a decay time of 25 years in the unsaturated zone is considered. Hence, at least at well SLP4 with a $^3He_{trit}$ concentration of 0.7 TU some loss of ^{3}He has to be

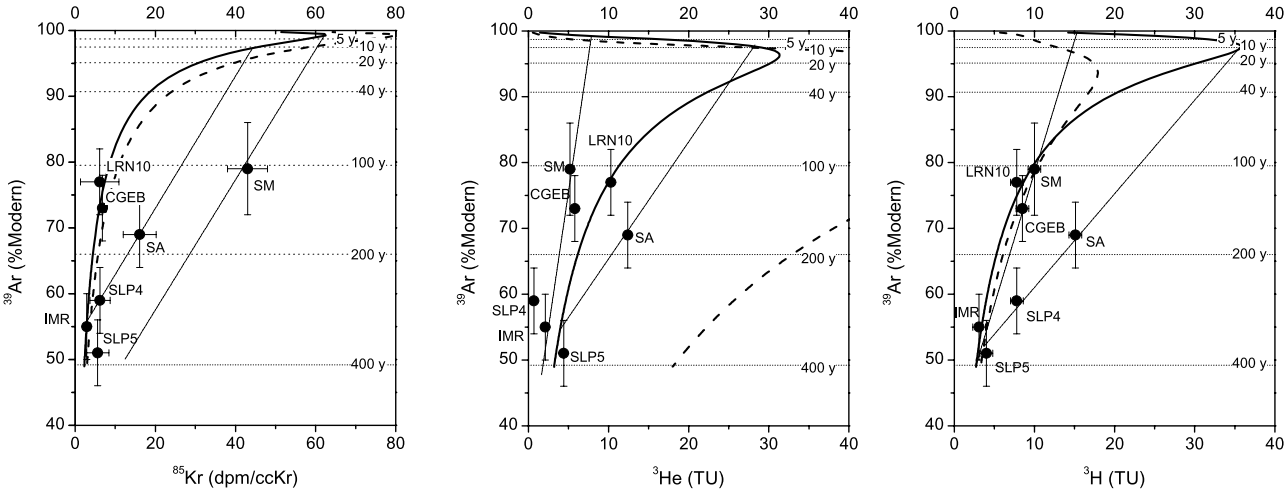

Figure 7. Argon 39 as function of the ^{85}Kr, ^{3}He, and ^{3}H concentrations. The plotted curves correspond to a one component groundwater where the whole water mass follows the EM (m = 1). The calculations are based on the atmospheric input (dashed line) and the input values calculated for a water table at 35 m depth (solid line). The dotted lines represent mixing lines between selected end-members which explain the measured data in SM and SA. The horizontal dotted lines indicate ^{39}Ar activities equivalent to EM ages of 5, 10, 20, 40, 100, 200, and 400 years.

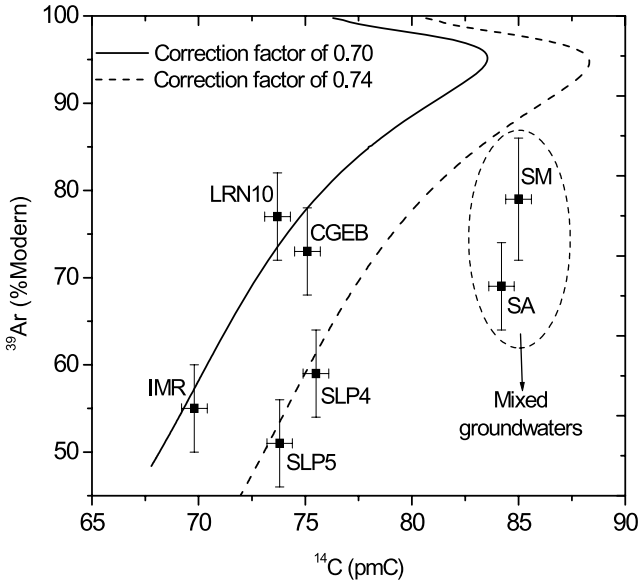

Figure 8. Argon 39 versus ^{14}C measured activities. The curves represent the tracer concentrations calculated with an EM for mean residence times ranging between 0 and 400 years. It is assumed that the dilution of the ^{14}C activity is similar for all the groundwaters in the range of ages (experimental correction factors 0.70–74). Atmospheric bomb-derived ^{14}C values were taken from *Levin and Kromer* [1997].

assumed. Previous studies have shown that $^{3}He_{tri}$ confinement is a function of the vertical flow velocity (recharge rate) and dispersivity. Hence significant $^{3}He_{tri}$ loss (>25%) can be expected at vertical flow velocities of less than 0.25 m/yr [*Schlosser et al.*, 1989]. The Fontainebleau Sands Aquifer is recharging at a rate of about 100–200 mm/yr (vertical water velocity of 0.4–0.8 m/yr); therefore a high confinement of $^{3}He_{tri}$ can be expected. The analyses of all five noble gas concentrations (He, Ne, Ar, Kr and Xe) measured in the aquifer, including $^{22}Ne/^{20}Ne$ and $^{40}Ar/^{36}Ar$ isotope ratios, indicated that some partial degassing may have led to a maximum loss of 28% of the originally dissolved excess air ^{3}He. In this case, the calculated $^{3}He_{tri}$ of SLP4 and IMR would be increased by about 0.6 TU; but the deviation of the measured $^{3}He_{trit}$ concentration from the expected values is as high as 3 TU. Hence the ^{3}He loss from the saturated zone appeared to be only partly responsible for the relatively depleted ^{3}He concentrations observed.

4.3. Additional Constrains to the Age Distribution: ^{14}C and ^{13}C Data

[50] Groundwater from the investigated wells in the Fontainebleau Sands Aquifer are highly mixed, and the models commonly used for the interpretation of ^{14}C in DIC (e.g., the model of Fontes-Garnier [*Fontes*, 1992]) do not account for this process. It should be also added that DIC in groundwater has different origins (e.g., root respiration, dead organic matter, rock carbonates, etc.); consequently the interpretation of the ^{14}C data is rather complex. Nevertheless, taking into account that the carbonates content in the aquifer is very homogeneous it can be assumed that the dilution of the initial ^{14}C activity is similar for all water components in the age range 0–400 years. Then, the course of ^{14}C according to the EM can be calculated, if the dilution factor is known. For our aquifer, an average dilution factor equal to 0.73 is estimated using geochemical mass balance modeling according to the model of Fontes and Garnier [*Fontes*, 1992]. (Water chemistry was taken from the BASELINE report (European Union, Natural baseline quality in European aquifers—A basis for aquifer management, EC Framework V Project, EVK1-CT1999-0006): (1) an average $\delta^{13}C_{CO2(g)}$ value of −25‰ for the soil CO_2 [*Gillon et al.*, 2004], (2) an assumed ^{14}C activity of 100 pmC for soil CO_2, and (3) a δ^{13}C and a ^{14}C activity in carbonate minerals from the rock matrix equal to 0‰ and 0 pmC, respectively.) The ^{39}Ar and ^{14}C data agree within uncertainties with the EM for dilution factors between 0.70 and 0.74 (Figure 8), in agreement with the geochemical modeling. No agreement was observed for the samples SA and SM (Figure 8). For the latter an at least two component mixing has to be assumed in accordance with the findings in the previous section. The consistency of ^{39}Ar and ^{14}C in the frame of the EM implies also absence of significant amounts of waters from the underlying Eocene aquifer. These last waters are much older, with depleted ^{14}C activities of <10 pmC [*Schneider et al.*, 2004].

5. Summary and Conclusions

[51] Data of five different environmental tracers with distinct half-lives and input functions were used in order to constrain the age distribution of groundwater samples taken from the Fontainebleau Sands Aquifer. In the saturated zone all tracers are transported in a similar way while in the unsaturated part of the aquifer the individual tracers behave very differently. This is in particular relevant for the young residence time indicators ^{3}H, ^{3}He and ^{85}Kr. Tritium is mainly transported advectively in the water phase, ^{85}Kr passes the unsaturated zone diffusively and $^{3}He_{trit}$ produced by decay of ^{3}H is lost to the atmosphere. Hence for the interpretation of environmental tracer data in terms of groundwater residence times it is crucial to consider in the present study that (1) a thick unsaturated soil zone is overlying the aquifer, and it delays water and tracer transport from the atmosphere to the water table and (2) samples were taken from large screened borehole intervals intercepting the water table in an area with spatially distributed recharge. Each water sample is therefore a mixture of waters with different ages. According to the hydrological situation it can be expected that the overall age distribution follows an exponential function [*Zuber*, 1986].

[52] The sensitivity to describe the overall age distribution of a water sample relies on the tracer method selected and on the mean age and spreading of the age distribution. If a large fraction of the water is younger than 50 years the transient tracers are the most sensitive tools. This is not the case in this study. Strong mixing and a mean residence time exceeding 50 years reduce the fraction of water that can be "seen" by the young residence time indicators. It raises the question in how far dating results from transient tracers can be extrapolated to the old part of the age distribution and how unimodal and multimodal age distributions can be distinguished. In the present study, the transient tracers failed to describe the whole age distribution of the sampled groundwater. In five boreholes, they predicted bimodal age distributions which were not confirmed with ^{39}Ar. Never-

theless, when ^{3}He was neglected from the fitting routine, unimodal age distributions were obtained.

[53] Tritium, ^{3}He, and ^{85}Kr were interpreted applying an inverse fitting procedure using conventional box models coupled with a tracer transport model trough the unsaturated soil. The box model parameters mean residence time (T_m) and portion of young water (m) were fitted for each individual sample whereas parameters characterizing the flow type (Pe and η) were assumed to be valid for all of the wells. The same supposition was made for transport in the unsaturated zone where the best fit mean recharge depth Z and recharge rate q_l were determined using the data from all of the wells. This procedure is different from the commonly adopted way of interpretation were tracer ages are compared. Here we characterize transit time distributions and/or model parameters by fitting to tracer concentrations. Tracer input functions at the water table assuming a mean unsaturated zone thickness of 35 m yielded the best agreement between modeled and measured tracer concentrations. The estimated recharge rate in the area of investigation of 100–150 mm/yr is in excellent agreement with previous values given in the literature. Several box models were tested and checked for consistency with the data. The best results could be obtained with the EM or the EPFM and the DM with model parameters that approximate the EM (η close to 1 for the EPFM and small Pe for the DM). This is in good agreement with the expectation. More surprising was the finding that in 5 samples best fits were obtained with mixing parameters m significantly smaller than one. This implies that an at least bimodal age distribution with considerable portions of prebomb water which are older than about 50 years have to be assumed for those samples according the ^{3}H/^{3}He and ^{85}Kr data. In two cases a strong correlation between mean residence time and mixing fraction was observed and the age distribution could not further be constrained applying the young residence time indicators alone.

[54] The ^{39}Ar measurements were used in order to check how far these dating results of the young residence time indicators are representative for the older tail (>50 years) of the age distribution. In only two of the samples a bimodal age distribution with a 300–400 years old water component was clearly confirmed. In the two above mentioned cases where some parameters are not independent, ^{39}Ar could reduce the range of parameters. (T_m: ~120 and ~400 years).

[55] In the other cases $^3He_{trit}$ concentrations were too low to be in agreement with the one component EM and also too low to be explained by a multimode age distribution. Therefore degassing of $^3He_{trit}$ is at least partly responsible for this disagreement. The high sensitive of ^{3}He to variations of the thickness of the unsaturated soil zone may also explain the larger scatter of the data. The ^{3}H/^{3}He ratios have therefore to be interpreted with care when the mean water residence time exceeds 50 years [*Waugh et al.*, 2003] and transport times in the saturated zone become large.

[56] ^{14}C data were used in a twofold way to further constrain or confirm the age distribution. Geochemical reactions affecting the atmospheric ^{14}C input occur homogeneously in the unsaturated and the saturated siliceous sands aquifer. The ^{14}C dilution factor is similar for all water components of the age spectra and was estimated experimentally to be between 0.70 and 0.74. This dilution factor is within uncertainties in agreement with expectations from geochemical modeling, which indicates that any ^{14}C reduction in DIC in water due to decay must be small. This means that very old water components (>1000 years) are absent. The remaining bomb derived ^{14}C was used as an additional tracer for young groundwater components and confirmed in general the findings from ^{3}H, ^{3}He, and ^{85}Kr.

[57] In summary, we show how multitracer data sets can be interpreted in an integrative way in order to investigate the age distribution of groundwater. Inverse modeling techniques allow the estimation of model parameters and their uncertainties. It is also shown that gas tracers such as ^{85}Kr (and SF_6 and CFCs) with steadily increasing input function and relatively short transfer times trough the unsaturated soil zone are less sensitive to pronounced mixing and unsaturated zone transport. However, reliable dating of groundwater with mean residence times older than 100 years requires a tracer with a longer half live.

Appendix A: The ^{37}Ar and ^{39}Ar Subsurface Production

[58] In the atmosphere ^{39}Ar is mainly produced by the reaction ^{40}Ar(n, 2n)^{39}Ar and decays with a half-life of 269 years with ^{39}K as decay product. Since nuclear weapon tests have not influenced the atmospheric ^{39}Ar activity, the infiltrating water exhibits a constant ^{39}Ar activity of 100% modern (0.107 ± 0.004 dpm/L Argon) [*Lehmann and Loosli*, 1984]. A possible limitation of the application of ^{39}Ar arises from the presence of subsurface produced ^{39}Ar [*Loosli and Lehmann*, 1989]. Such ^{39}Ar is mainly the result of the interaction of neutrons with ^{39}K atoms in the rock matrix. A high ^{39}Ar production rate requires (1) high U and Th concentrations in the rock, (2) low concentration of n absorbing elements in the rock (Gd, B, etc.), (3) high K concentration in the rock, and (4) a high escape rate from rock into the water phase. Such conditions (in particular 1) were, e.g., fulfilled in the Stripa granite in Sweden, where the mean concentrations of uranium and thorium in the rocks were 44.1 and 33.0 ppm respectively. Activity values of ^{39}Ar higher than 1000% modern were measured [*Andrews et al.*, 1989]. However in many aquifers with average crustal U and Th concentrations of ~2 and 6–10 ppm, respectively, ^{39}Ar activities below or at the detection limit can be expected [*Bath et al.*, 1978; *Loosli*, 1983; *Purtschert et al.*, 2001b].

[59] Lacking ^{39}Ar free old waters in the investigated aquifer, which would indicate negligible subsurface production, one has two alternative methods to estimate the order of magnitude of subsurface production. A first method is based on the use of ^{37}Ar. Argon 37 is also produced by subsurface neutrons by the ^{40}Ca(n, α)^{37}Ar reaction and its short half-life of 35 days excludes any atmospheric component in old groundwater. Argon 37 is therefore a good monitor for subsurface n fluxes. However, because the target elements K and Ca are elements of different rock minerals with probably different grain sizes and microscopic structure, a large uncertainty of the relative release rates of ^{39}Ar and ^{37}Ar remains. Similar problems are encountered when ^{37}Ar measurements are replaced or complemented with theoretical simulations of the subsur-

Table A1. Results of the Measurements of ^{37}Ar and ^{39}Ar in Samples From the Well IMR[a]

Isotope	Measured Values Activity	Calculated Values[b]			
		Equilibrium Concentration in Rock [atoms/cm^3 rock]	Concentration in Water [atoms/g water]	Concentration of Argon [cm^3 STP/g water]	Activity in Water
^{37}Ar	<0.027 dpm/L Ar	$\sim 1 \times 10^{-6}$	4×10^{-9} to 4×10^{-7}	$(4.33 \pm 0.03) \times 10^{-4}$	10^{-7} to 10^{-5} dpm/L Ar
^{39}Ar	(55 ± 5)% modern	1.3	0.005 to 0.520	$(4.33 \pm 0.03) \times 10^{-4}$	0.05 to 5.5% modern

[a]The ^{37}Ar and ^{39}Ar equilibrium concentrations in rocks, calculated from neutron production rates, and rock chemical composition are also given.
[b]Calculations were made assuming the following data: uranium and thorium concentrations of 0.59 and 1.25 ppm, respectively; escape factors from rocks to the water phase between 0.1 and 10% [*Loosli et al.*, 1991] and a saturated porosity of 25%.

face neutron fluxes and production rates of ^{37}Ar and ^{39}Ar [*Lehmann and Loosli*, 1991].

[60] In the present study, the subsurface production of ^{39}Ar was estimated using both methods. On the basis of the measured mean rock composition, an estimated (large) range of escape rates e of ^{37}Ar and ^{39}Ar between 0.1 and 10% [*Loosli et al.*, 1991] and a rock porosity p of 25% [*Mercier*, 1981] equilibrium concentrations of ^{37}Ar and ^{39}Ar in the rock matrix (N_R) and in the water N_W were calculated using the relationship:

$$N_w = N_R \cdot \frac{e}{p} \tag{A1}$$

[61] Upper limits of the subsurface produced activities (e = 10%) are 10^{-5} dpm/L Ar and 6% modern for ^{37}Ar and ^{39}Ar, respectively (Table A1). The low calculated value for ^{37}Ar is in agreement with the measured activity in well IMR which is below the detection limit of 0.03 dpm/L Ar (for comparison ^{37}Ar in Stripa groundwater is between 2 and 13 dpm/L Ar [*Loosli et al.*, 1989]). It can be concluded that the calculated upper limit of ^{39}Ar of 6% modern is also valid. Because this value is comparable to the detection limit (5% modern), subsurface produced ^{39}Ar was neglected in the dating calculations in the Fontainebleau Sands Aquifer.

Appendix B: Noble Gases

[62] The noble gas data were interpreted by fitting various models for noble gas dissolution in groundwater to the concentrations of the atmospheric gases (Ne, Ar, Kr, Xe) in order to determine the model parameter values that minimize the error weighted deviation (measured by χ^2, compare equation (2) and the work by *Aeschbach-Hertig et al.* [1999]). This procedure yielded very good fits with the simplest model, assuming that the excess of the concentrations above solubility equilibrium (excess air) is pure atmospheric air (unfractionated air or UA model). The low values of χ^2 (and correspondingly high values of the probability of finding these values according to a χ^2 distribution with 2 degrees of freedom) suggest that the above model describes the measured concentrations very well and that, for example, no degassing in the aquifer or in the samples has occurred.

[63] However, if the derived model parameters are applied for He, and the difference between measured He concentrations and modeled atmosphere-derived He concentrations is interpreted as the radiogenic He component, small but significant negative values are calculated for the radiogenic He in all cases (Table 5). The model predicts between 2 and 6% more helium than measured. The problem of apparently negative radiogenic He concentrations is quite frequently encountered in studies applying ^{3}H-^{3}He dating to shallow groundwater, when the atmospheric He is estimated from the measured Ne concentration [*Peeters et al.*, 2002b]. The usually adopted solution for the calculation of the tritiogenic ^{3}He component is to assume that the radiogenic He concentrations are equal to zero. The tritiogenic ^{3}He and hence the ^{3}H-^{3}He age can then be calculated using only the measured He data and the equilibration temperature (NGT) derived from the other noble gases. The tritiogenic ^{3}He concentrations listed in table 3 and the ^{3}H-^{3}He ages in Table 4 were calculated in this way.

[64] The physically senseless result of negative radiogenic He concentrations indicates that the model used to fit the heavy noble gases is incomplete. Such a discrepancy can be explained by a fractionation of the excess air relative to air, as discussed by *Peeters et al.* [2002b]. Two fractionation models are commonly used (see *Kipfer et al.* [2002] for a review): the CE model, assuming incomplete dissolution of entrapped air bubbles and closed system equilibration [*Aeschbach-Hertig et al.*, 2000] and the PR model, assuming partial diffusive reequilibration [*Stute et al.*, 1995]. Both models can in principle resolve the problem by introducing a fractionation parameter $F > 0$. However, the fitting procedure based only on Ne, Ar, Kr, and Xe always yields best fits for $F = 0$, corresponding to unfractionated excess air. Therefore this approach does not provide a unique and consistent solution.

[65] Adopting the assumption that no radiogenic He is present allows finding a unique and consistent interpretation for all noble gases. With this assumption, He can be treated as a purely atmospheric gas and included in the fitting procedure along with the other noble gases. With He as an additional constraint, the UA model does not provide acceptable fits ($p < 0.01$) for 3 of the seven samples. The CE model does not perform significantly better. However, the PR model still yields very good fits, with small values of the fractionation parameter ($F < 0.17$). The derived NGTs with this fit are slightly (0.04 to 0.20 °C) higher than those derived only from the heavy noble gases (Table 3), but the difference is within the uncertainty of the fitting results. The tritiogenic ^{3}He concentrations calculated with this model differ slightly from those calculated from He only (Table 5).

[66] The finding that only the PR model explains all measured noble gas concentrations is rather surprising, since several previous studies have argued for the use of the CE model [*Aeschbach-Hertig et al.*, 2000; *Peeters et al.*, 2002a, 2002b]. *Peeters et al.* [2002a] showed that the isotope ratios of Ne and Ar can provide a clear test for the applicability of the PR model. Therefore, as a final

consistency check, the fitting procedure was performed using all five noble gas concentrations and the $^{22}Ne/^{20}Ne$ (0.102) and $^{40}Ar/^{36}Ar$ (295.5) ratios as constraints. The PR model remains the favored model in this case and still yields a good explanation of all measured data. However, it should be noted that the isotope ratios do not provide strong constraints in the present case of weak fractionation.

[67] The $^3He_{tri}$ concentrations in groundwater vary between 1.1×10^{-14} and 5.2×10^{-14} cm^3 He STP per g of water (Table 5). The noble gas temperatures (NGT) range between 9.6° and 10.6°C, with errors of approximately 0.2°C, and correspond within the range of measured variation (~1°C) to the present interannual mean air temperature of 11.0 ± 0.6°C (Meteo France, Trappes station, 1991–2000). Excess air concentrations, expressed as the excess of Ne in the sample compared to the equilibrium concentration (ΔNe) range between 30 and 59%.

[68] **Acknowledgments.** This study was partially supported by the EU project BASELINE "Natural Baseline Quality of European Groundwaters: A Basis for Aquifer Management." We would like to thank three anonymous reviewers for their helpful comments.

References

Aeschbach-Hertig, W., F. Peeters, U. Beyerle, and R. Kipfer (1999), Interpretation of dissolved atmospheric noble gases in natural waters, *Water Resour. Res.*, *35*, 2779–2792.

Aeschbach-Hertig, W., F. Peeters, U. Beyerle, and R. Kipfer (2000), Palaeotemperature reconstruction from noble gases in ground water taking into account equilibration with entrapped air, *Nature*, *405*, 1040–1044.

Andrews, J. N., W. Balderer, A. H. Bath, H. B. Clausen, G. V. Evans, T. Florkowski, J. E. Goldbrunner, M. Ivanovich, H. H. Loosli, and H. Zojer (1984), Environmental isotope studies in two aquifer systems: A comparison of groundwater dating methods, in *Isotope Hydrology 1983*, pp. 535–577, Int. At. Energy Agency, Vienna.

Andrews, J. N., S. N. Davis, J. Fabryka-Martin, J.-C. Fontes, B. E. Lehmann, H. H. Loosli, J.-L. Michelot, H. Moser, B. Smith, and M. Wolf (1989), The in situ production of radioisotopes in rock matrices with particular reference to the Stripa Granite, *Geochim. Cosmochim. Acta*, *53*, 1803–1815.

Bariteau, A. (1996), Modélisation géochimique d'un aquifère: La nappe de l'Oligocène en Beauce et l'altération des Sables de Fontainebleau, thesis, Ecole des Mines de Paris, Paris.

Barraclough, P. B., and P. B. Tinker (1982), The determination of ionic diffusion coefficients in field soils. II. Diffusion of bromide ions in undisturbed soil cores, *J. Soil Sci.*, *33*, 13–24.

Bath, A. H., W. M. Edmunds, and J. N. Andrews (1978), Palaeoclimatic trends deduced from the hydrochemistry of a Triassic sandstone aquifer, United Kingdom, in *Isotope Hydrology*, pp. 545–568, Int. At. Energy Agency, Vienna.

Bergonzini, L. (2000), Caractérisation géochimique de la nappe des Sables de Fontainebleau, paper presented at 18th Réunion des Sciences de la Terre, Soc. Géol. de Fr., Paris.

Beyerle, U., R. Purtschert, W. Aeschbach-Hertig, D. M. Imboden, H. H. Loosli, R. Wieler, and R. Kipfer (1998), Climate and groundwater recharge during the last glaciation in an ice-covered region, *Science*, *282*, 731–734.

Beyerle, U., W. Aeschbach-Hertig, D. M. Imboden, H. Baur, T. Graf, and R. Kipfer (2000), A mass spectrometric system for the analysis of noble gases and tritium from water samples, *Environ. Sci. Technol.*, *34*, 2042–2050.

Busenberg, E., and L. N. Plummer (1992), Use of chlorofluorocarbons (CCl_3F and CCl_2F_2) as hydrologic tracers and age-dating tools: The alluvium and terrace system of central Oklahoma, *Water Resour. Res.*, *28*, 2257–2283.

Carrera, J., A. Alcolea, A. Medina, J. Hidalgo, and L. J. Slooten (2005), Inverse problem in hydrogeology, *Hydrogeol. J.*, *13*, 206–222.

Cook, P. G., and D. K. Solomon (1995), Transport of atmospheric trace gases to the water table: Implications for groundwater dating with chlorofluorocarbons and krypton-85, *Water Resour. Res.*, *31*, 263–270.

Coplen, T. B., A. L. Herczeg, and C. Barnes (1999), Isotope engineering—Using stable isotopes of the water molecule to solve practical problems, in *Environmental Tracers in Subsurface Hydrology*, edited by P. G. Cook and A. L. Herczeg, pp. 79–110, Springer, New York.

Corcho Alvarado, J. A., R. Purtschert, F. Barbecot, C. Chabault, J. Rüedi, V. Schneider, W. Aeschbach-Hertig, R. Kipfer, and H. H. Loosli (2004), Tracer transport in the unsaturated zone of the Fontainebleau Sands Aquifer, paper presented at International Workshop on the Application of Isotope Techniques in Hydrological and Environmental Studies, Int. At. Energy Agency, Paris.

Fontes, J. C. (1992), Chemical and isotopic constraints on ^{14}C dating of groundwater, in *Radiocarbon After Four Decades*, edited by R. E. Taylor, A. Long, and R. S. Kra, pp. 242–261, Springer, New York.

Fontes, J. C., and J. M. Garnier (1979), Determination of the initial ^{14}C activity of the total dissolved carbon: A review of the existing models and a new approach, *Water Resour. Res.*, *15*, 399–413.

Forster, M., K. Ramm, and P. Maier (1992), Argon-39 dating of groundwater and its limiting conditions, in *Isotope Techniques in Water Resource Development 1991*, pp. 203–214, Int. At. Energy Agency, Vienna.

Gaye, C. B., and W. M. Edmunds (1996), Groundwater recharge estimation using chloride, stable isotopes and tritium profiles in the sands of northwestern Senegal, *Environ. Geol.*, *27*, 246–251.

Gillon, M., F. Barbecot, E. Gibert, C. Marlin, and M. Massault (2004), Variability of CO_2 composition in ^{13}C within the unsaturated zone and influence on groundwater dating, paper presented at International Workshop on the Application of Isotope Techniques in Hydrological and Environmental Studies, Int. At. Energy Agency, Paris.

Kalin, R. M. (1999), Radiocarbon dating of groundwater systems, in *Environmental Tracers in Subsurface Hydrology*, edited by P. G. Cook and A. L. Herczeg, pp. 111–144, Springer, New York.

Kipfer, R., W. Aeschbach-Hertig, F. Peeters, and M. Stute (2002), Noble gases in lakes and ground waters, in *Noble Gases in Geochemistry and Cosmochemistry*, *Rev. Mineral. Geochem.*, vol. 47, edited by D. Porcelli, C. Ballentine, and R. Wieler, pp. 615–700, Mineral. Soc. of Am., Washington, D. C.

Lehmann, B., and H. H. Loosli (1984), Use of noble gas radioisotopes for environmental research, in *Resonance Ionization Spectroscopy 1984*, *Conf. Ser.*, vol. 71, pp. 219–226, Inst. of Phys., Bristol, U. K.

Lehmann, B. E., and H. H. Loosli (1991), Isotopes formed by underground production, in *Applied Isotope Hydrogeology: A Case Study in Northern Switzerland*, edited by F. J. Pearson et al., pp. 239–296, Elsevier, New York.

Levin, I., and B. Kromer (1997), $\delta^{14}CO_2$ records from Schauinsland, in *Trends: A Compendium of Data on Global Change*, Carbon Dioxide Inf. Anal. Cent., Oak Ridge Natl. Lab., Oak Ridge, Tenn. (Available at http://cdiac.ornl.gov/trends/co2/cent-scha.htm)

Loosli, H. H. (1983), A dating method with ^{39}Ar, *Earth Sci. Planet. Lett.*, *63*, 51.

Loosli, H. H., and B. E. Lehmann (1989), Transfer of underground produced ^{37}Ar, ^{39}Ar and ^{40}Ar from rock into water, in *Water-Rock Interaction WRI-6*, pp. 445–448, A. A. Balkema, Brookfield, Vt.

Loosli, H. H., M. Moeli, H. Oeschger, and U. Schotterer (1986), Ten years low-level counting in the underground laboratory in Bern, Switzerland, *Nucl. Instr. Methods Phys. Res., Sect. B*, *17*, 402–405.

Loosli, H. H., B. E. Lehmann, and W. Balderer (1989), Argon-39, argon-37 and krypton-85 isotopes in Stripa groundwaters, *Geochim. Cosmochim. Acta*, *53*, 1825–1829.

Loosli, H. H., B. E. Lehmann, and G. Däppen (1991), Dating by radionuclides, in *Applied Isotope Hydrogeology: A Case Study in Northern Switzerland*, edited by F. J. Pearson et al., pp. 153–174, Elsevier, New York.

Loosli, H. H., B. E. Lehmann, C. Thalmann, J. N. Andrews, and T. Florkowski (1992), Argon-37 and argon-39: Measured concentrations in groundwater compared with calculated concentrations in rock, in *Isotope Techniques in Water Resources Development*, pp. 189–201, Int. At. Energy Agency, Vienna.

Loosli, H. H., B. E. Lehmann, and W. M. Smethie (1999), Noble gas radioisotopes: ^{37}Ar, ^{85}Kr, ^{39}Ar, ^{81}Kr, in *Environmental Tracers in Subsurface Hydrology*, edited by P. G. Cook and A. L. Herczeg, pp. 379–396, Springer, New York.

Mazor, E. (1972), Paleotemperatures and other hydrological parameters deduced from noble gases dissolved in groundwaters, Jordan Rift Valley, Israel, *Geochim. Cosmochim. Acta*, *36*, 1321–1336.

Mégnien, C. (1979), Hydrogéologie du centre du Bassin de Paris, *Mem. BRGM*, *98*, 144–149.

Ménillet, F. (1988), Meulières, argiles à meulières et meuliérisation—Historique évolution des termes et hypothèses génétiques, *Bull. Inf. Geol. Bassin Paris*, *25*(4), 71–79.

Mercier, R. (1981), Inventaire des ressources aquifères et vulnérabilité des nappes du département des Yvelines, *Rapp. 81SGN348IDF*, Bur. de Rech. Géol. et Min., Paris.

Millington, R. J. (1959), Gas diffusion in porous media, *Science*, *130*, 100–102.

Mook, W. G. (1980), Carbon-14 in hydrogeological studies, in *Handbook of Environmental Isotope Geochemistry*, vol. 1, edited by P. Fritz and J. C. Fontes, pp. 49–74, Elsevier, New York.

Oeschger, H., A. Gugelman, H. H. Loosi, U. Schotterer, U. Siegenthaler, and W. Wiest (1974), ^{39}Ar dating of groundwater, in *Isotope Techniques in Groundwater Hydrology*, pp. 179–190, Int. At. Energy Agency, Vienna.

Pearson, F. J., Jr., W. Balderer, H. H. Loosli, B. E. Lehmann, A. Matter, T. Peters, H. Schmassmann, and A. Gautschi (1991), *Applied Isotope Hydrology: A Case Study in Northern Switzerland*, 436 pp., Elsevier, New York.

Peeters, F., U. Beyerle, W. Aeschbach-Hertig, J. Holocher, M. S. Brennwald, and R. Kipfer (2002a), Improving noble gas based paleoclimate reconstruction and groundwater dating using ^{20}Ne/^{22}Ne ratios, *Geochim. Cosmochim. Acta*, *67*, 587–600.

Peeters, F., W. Aeschbach-Hertig, J. Holocher, and R. Kipfer (2002b), Excess air correction in groundwater dating with He isotopes, Goldschmidt conference, Davos, Switzerland, *Geochim. Cosmochim. Acta*, *67*, A587.

Plummer, L. N., and E. Busenberg (1999), Chlorofluorocarbons, in *Environmental Tracers in Subsurface Hydrology*, edited by P. G. Cook and A. L. Herczeg, pp. 441–478, Springer, New York.

Poeter, E. P., and M. C. Hill (1997), Inverse methods: A necessary next step in groundwater modeling, *Ground Water*, *35*(2), 250–260.

Poreda, R. J., T. E. Cerling, and D. K. Solomon (1988), Tritium and helium isotopes as hydrologictracers in a shallow unconfined aquifer, *J. Hydrol.*, *103*, 1–9.

Press, W. H., P. F. Flannery, S. A. Teukolsky, and W. T. Vetterling (1986), *Numerical Recipes*, 818 pp., Cambridge Univ. Press, New York.

Purtschert, R., B. E. Lehmann, and H. H. Loosli (2001a), Groundwater dating and subsurface processes investigated by noble gas isotopes (^{37}Ar, ^{39}Ar, ^{85}Kr, ^{222}Rn, ^{4}He), in *Water Rock Interaction, WRI-10*, vol. 2, edited by R. Cidu, pp. 1569–1573, A. A. Balkema, Brookfield, Vt.

Purtschert, R., W. Aeschbach-Hertig, U. Beyerle, R. Kipfer, and H. H. Loosli (2001b), Palaeowaters from the Glatt Valley, Switzerland, in *Palaeowaters in Coastal Europe: Evolution of Groundwater Since the Late Pleistocene*, edited by W. M. Edmunds and C. J. Milne, *Geol. Soc. Spec. Publ.*, *189*, 155–162.

Rampon, G. (1965), Etat de la documentation sur les ouvrages souterrains implantés sur les feuilles topographiques de Nogent le Roi-Rambouillet et synthèse hydrogéologique proviso ire, *Rapp. DSGR. 65.A7*, Bur. des Rech. Géol. et Min., Paris.

Roether, W. (1967), Estimating the tritium input to groundwater from wine samples: Groundwater and direct run-off contribution to central European surface waters, in *Isotopes in Hydrology*, pp. 73–79, Int. At. Energy Agency, Vienna.

Rueedi, J., M. S. Brennwald, R. Purtschert, U. Beyerle, M. Hofer, and R. Kipfer (2005), Estimating amount and spatial distribution of groundwater recharge in the Illumeden basin (Niger) based on ^{3}H, ^{3}He, and CFC-11 measurements, *Hydrol. Processes*, *19*(17), 3285–3298.

Schlosser, P., M. Stute, H. Dorr, C. Sonntag, and K. O. Munnich (1988), Tritium/^{3}He dating of shallow groundwater, *Earth Planet. Sci. Lett.*, *89*, 353–362.

Schlosser, P., M. Stute, C. Sonntag, and K. O. Munnich (1989), Tritiogenic ^{3}He in shallow groundwater, *Earth Planet. Sci. Lett.*, *94*, 245–256.

Schneider, V. (2005), Apports de l'hydrodynamique et de la géochimie à la caractérisation des nappes de lOligocène et de lÉocene, et à la reconnaissance de leurs relations actuelles et passées: Origine de la dégradation de la nappe de lOligocène (sud-ouest du Bassin de Pris), Ph.D. thesis, Univ. Paris-Sud, Orsay, France.

Schneider, V., F. Barbecot, L. Bergonzini, C. Marlin, A. Filly, M. Massault, and L. Dever (2004), Geochemical-hydrological relationships between two groundwater bodies of the Paris Basin: Clues for a conceptual model, paper presented at International Workshop on the Application of Isotope Techniques in Hydrological and Environmental Studies, Int. At. Energy Agency, Paris.

Smethie, W. M., Jr., D. K. Solomon, S. L. Schiff, and G. G. Mathieu (1992), Tracing groundwater flow in the Borden Aquifer using krypton-85, *J. Hydrol.*, *130*, 279–297.

Solomon, D. K., and P. G. Cook (1999), ^{3}H and ^{3}He, in *Environmental Tracers in Subsurface Hydrology*, edited by P. G. Cook and A. L. Herczeg, pp. 397–424, Springer, New York.

Stute, M., and P. Schlosser (1999), Atmospheric noble gases, in *Environmental Tracers in Subsurface Hydrology*, edited by P. G. Cook and A. L. Herczeg, pp. 349–377, Springer, New York.

Stute, M., P. Schlosser, J. F. Clark, and W. S. Broecker (1992), Paleotemperatures in the southwestern United States derived from noble gas measurements in groundwater, *Science*, *256*, 1000–1003.

Stute, M., M. Forster, H. Frischkorn, A. Serejo, J. F. Clark, P. Schlosser, W. S. Broecker, and G. Bonani (1995), Cooling of tropical Brazil (5°C) during the Last Glacial Maximum, *Science*, *269*, 379–383.

Vernoux, J. F., Y. M. Le Nindre, and J. C. Martin (2001), Relations nappe-rivière et impact des prélèvements d'eau souterraine sur le débit des cours d'eau dans le bassin de la Juine et de l'Essonne, *Rapp. BRGM/RP-50637-FR*, Bur. de Rech. Géol. et Min., Paris.

Waugh, D. W., T. M. Hall, and T. W. N. Haine (2003), Relationship among tracer ages, *J. Geophys. Res.*, *108*(C5), 3138, doi:10.1029/2002JC001325.

Weissmann, G. S., Y. Zhang, E. M. LaBolle, and G. E. Fogg (2002), Dispersion of groundwater age in an alluvial aquifer system, *Water Resour. Res.*, *38*(10), 1198, doi:10.1029/2001WR000907.

Winger, K., J. Feichter, M. Kalinowski, H. Sartorius, and C. Sclosser (2005), A new compilation of the atmospheric ^{85}Krypton inventories from 1945 to 2000 and its evaluation in a global transport model, *J. Environ. Radioact.*, *80*, 183–215.

Zuber, A. (1986), Mathematical models for the interpretation of environmental radioisotopes in groundwater systems, in *Handbook of Environmental Isotope Geochemistry*, vol. 2, *The Terrestrial Environment B*, edited by P. Fritz and J. C. Fontes, pp. 1–59, Elsevier, New York.

Zuber, A., and P. Maloszewski (2001), Lumped-parameter models, in *Environmental Isotopes in the Hydrological Cycle*, vol. 6, *Modelling*, *Tech. Doc. Hydrol. 39*, pp. 5–35, Int. At. Energy Agency, Paris.

W. Aeschbach-Hertig, Institute of Environmental Physics, University of Heidelberg, D-69120 Heidelberg, Germany.

F. Barbecot, C. Chabault, and V. Schneider, Laboratoire Interactions et Dynamique des Environnements de Surface, UMR 8148 IDES, Bâtiment 504, Université Paris-Sud, F-91405 Orsay Cedex, France.

J. A. Corcho Alvarado, H. H. Loosli, and R. Purtschert, Climate and Environmental Physics Division, Physics Institute, University of Bern, Sidlerstrasse 5, CH-3012 Bern, Switzerland. (corcho@climate.unibe.ch)

R. Kipfer, Water Resources and Drinking Water, EAWAG, CH-8600 Dübendorf, Switzerland.

J. Rueedi, Robens Centre for Public and Environmental Health, University of Surrey, Guildford GU2 7XH, UK.